

RESEARCH

Open Access



Enhancement of terephthalic acid recovered from PET waste using a combination of citric acid and dimethyl sulfoxide extraction

Thi Hong Nguyen¹ and Kung-Yuh Chiang^{1*}

Abstract

This study aimed to develop an eco-friendly, cost-efficient, and practically viable method for extracting terephthalic acid (H₂BDC) from polyethylene terephthalic (PET) waste. Dimethyl sulfoxide (DMSO) was combined with either citric acid (C₆H₈O₇) or H₂SO₄ to enhance the particle size of H₂BDC, and the optimum conditions during the acidification step were determined. Additionally, response surface methodology was employed to examine the influence and interaction of extractant (NaOH) concentration, hydrolysis temperature, and time on the optimal H₂BDC yield and recovery ratio. Experimental results demonstrated that NaOH concentration significantly impacted both H₂BDC yield and recovery ratio, surpassing the effects of hydrolysis temperature and time. Under optimal conditions involving a temperature of 200 °C and a 12 h reaction time with 5% NaOH, the model predicted a 100% yield and recovery ratio, which closely matched the experimental results of 99% and 100% for yield and recovery ratio, respectively. To enhance particle size, a combination of DMSO and C₆H₈O₇ was more effective than H₂SO₄. The maximum particle size achieved was 57.4 μm under the following optimum conditions: premixing 5 M C₆H₈O₇ with DMSO at a 35:75 mL ratio and maintaining a reaction temperature of 75 °C for 40 min. The study demonstrated the stability and consistency of the method. The H₂BDC yield remained between 96 and 98% with high purity over eight consecutive cycles of using the DMSO and C₆H₈O₇ mixture. The findings highlight the importance of integrating C₆H₈O₇ and DMSO to enhance H₂BDC quality, meeting commercial product criteria with evidence of high purity and large particle size. This method presents a promising solution for extracting H₂BDC from PET waste, with potential implications for the recycling industry and a positive environmental impact.

Keywords Terephthalic acid, Polyethylene terephthalic (PET), Response surface methodology, Citric acid, Dimethyl sulfoxide

1 Introduction

Plastics have become one of the most widely used materials worldwide, significantly increasing plastic waste generation [1–3]. Regrettably, substantial waste finds its way into landfills and marine environments, causing

environmental concerns [2, 4]. In 2015 alone, a staggering 6.3 Bt of plastic waste was generated, with only a mere 9% recycling ratio. The rest either underwent incineration (12%) or ended up in landfills and oceans (up to 79%), exacerbating the environmental issues associated with plastic pollution [4–8]. If this trend persists, projections indicate that by 2050, as much as 12 Mt of plastic waste could enter landfills and natural habitats. The effectiveness of plastic waste recycling is significantly impacted by the collection, sorting, and waste processing procedures adopted by each country. Developed economies,

*Correspondence:

Kung-Yuh Chiang
kychiang@ncu.edu.tw

¹ Graduate Institute of Environmental Engineering, National Central University, Tao-Yuan City 30201, Taiwan



acid-DMSO mixture based on yield, particle size, and purity considerations.

2 Materials and methods

2.1 Materials

This study collected PET waste from household recycling bins in Taoyuan City, Taiwan, and was prepared for experimentation. The PET waste underwent a series of processes: initial drying in an oven at 90 °C for 24 h, followed by thorough washing with tap water. The chemicals employed in the experiment, TBAI, 1,4 benzene dicarboxylate, ethanol, and DMSO of 99.9% purity, were procured from Sigma-Aldrich. Citric acid monohydrate (99.9% purity), H₂SO₄, and NaOH were provided by Avantor Performance Materials Inc (Radnor, PA, US). Aqueous citric acid monohydrate, sulfuric acid, and sodium hydroxide solutions were prepared with Milli-Q water. All chemicals were used without the need for further purification. The PET waste's characteristics were thoroughly examined through proximate and ultimate analyses by Taiwan Environmental Protection Administration standards (NIEA R213 and R205). It encompassed the determination of moisture, ash content, volatile matter, and fixed carbon. This analytical procedure was carried out in triplicate to ensure accuracy and reliability. The ultimate analysis of PET samples was conducted using an elemental analyzer (Elementary Analyzer, Vario MICRO). As detailed in Table S1, the PET waste exhibited a notable carbon content, with a dominant presence

of approximately 57.8 ± 1.9%. The energy content of the PET samples was quantified using a bomb calorimeter (Parr 1341 calorimeter) following NIEA E214.01C protocol.

2.2 The extraction process of H₂BDC derived from PET waste

2.2.1 Alkaline hydrolysis process

The extraction procedure was undertaken in a dual-stage process encompassing hydrolysis and subsequent acidification, as illustrated in Fig. 1. For the hydrolysis phase, one gram of PET flakes was immersed in a mixture comprising varying quantities of NaOH (5, 10, and 15%) and distilled water (in mL). The mass ratio of NaOH to PET was set at 3:1, and for DI water to PET, it was maintained at 10:1. The hydrolysis procedure was conducted under two conditions: one without the incorporation of a catalyst, and the other involving the introduction of a phase-transfer catalyst named TBAI. The hydrolysis reaction was performed within a 50 mL Teflon-coated steel autoclave reactor. The reactor was subjected to different temperature conditions, specifically 160, 180, and 200 °C, and the reaction duration was set at 8, 10, and 12 h. The reactor was cooled to room temperature upon reaching the designated reaction time. 20% NaOH concentration was added to neutralize the mixture until the solution reached a pH of 14, ensuring complete dissolution of any remaining H₂BDC [36]. Subsequently, the unreacted

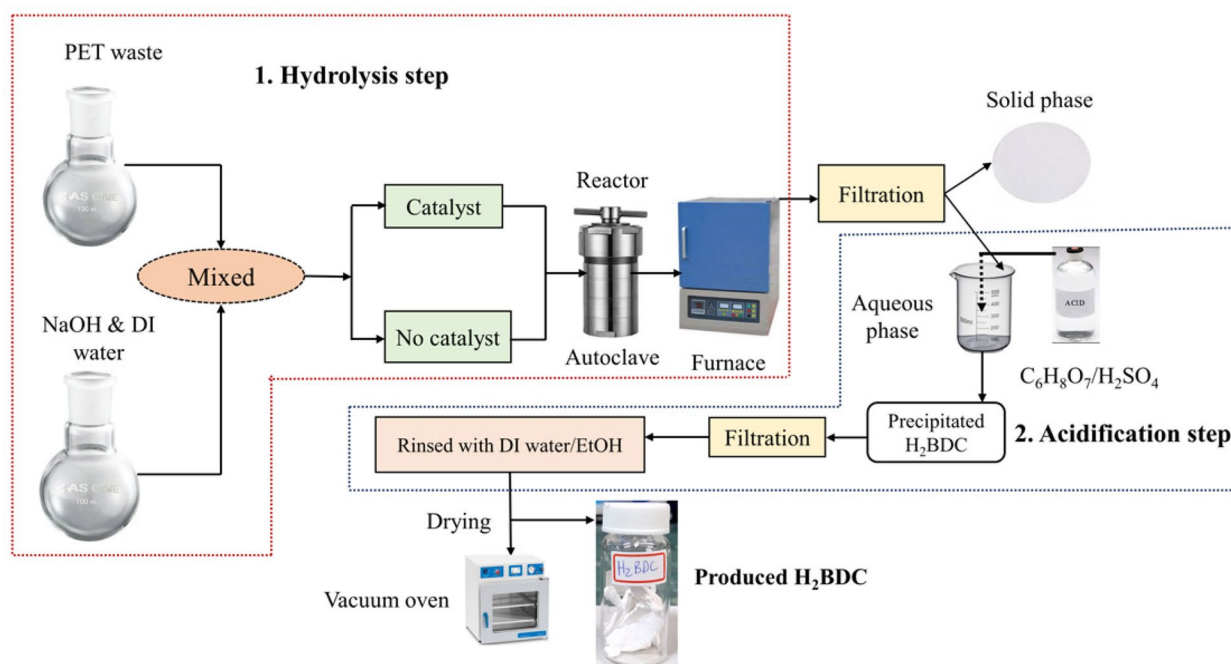


Fig. 1 A schematic diagram of PET-derived H₂BDC extraction procedure

solid phase of PET was separated from the mixture using vacuum filtration.

2.2.2 Acidification process and computation of H₂BDC production yield

The precipitation capability was determined by the acidification reactions separately using two different acid solutions, namely 4.5 M H₂SO₄ and C₆H₈O₇. H₂SO₄ was gradually added to the filtrate until the pH reached 1.0, following the approach outlined by Manju et al. in 2013 [37]. Previous research has not explored the precipitation of H₂BDC using C₆H₈O₇, and this led to our examination of various C₆H₈O₇ concentrations (1, 3, and 5 M) to determine the ideal concentration and final pH value for precipitation. The goal was to maximize the yield of H₂BDC and control particle size while minimizing acid consumption. The experiments were conducted with various pH values (2.5, 3.5, and 4.0) to determine the H₂BDC yield. Additionally, the efficacy of DMSO in enhancing H₂BDC particle size was evaluated. In this research, 5 M C₆H₈O₇ was combined with DMSO at different volume ratios (1:1, 1:2, and 1:3) while maintaining a pH of 4.0 in the experiments.

Further experiments involved mixing different concentrations of citric acid (1, 3, and 5 M) with DMSO and subjecting them to acidification at various reaction temperatures (25, 50, and 75 °C) and durations (5, 40, and 60 min). Throughout these experiments, the precipitation reactions were maintained at a constant stirring speed of 300 rpm. The resulting H₂BDC product was collected through filtration, washed with deionized (DI) water or ethanol (EtOH) and dried at 60 °C for 12 h in a vacuum oven [12]. The conversion percentage of PET and the yield percentage of H₂BDC were subsequently calculated. It is important to note that, following the precipitation reaction and the cooling process, the aqueous phase containing citric acid and DMSO solvent was separated through filtration. This aqueous phase was recycled for subsequent precipitation reactions, and its reusability was assessed regarding yield and particle size.

PET conversion and H₂BDC yield (%) were determined as follows: Eqs. (1) and (2):

$$\text{PET conversion (\%)} = \frac{(W_{\text{PET},i} - W_{\text{PET},f})}{W_{\text{PET},i}} \times 100\% \tag{1}$$

W_{PET,i} is the initial weight of PET and W_{PET,f} is the final weight of PET that remains on filter paper after filtration.

$$\text{Yield (\%)} = \frac{W_{\text{precipitate}}}{W_{\text{theoretical}}} \times 100\% \tag{2}$$

W_{theoretical} is the weight of H₂BDC recovered theoretically (100% recovery of 3 g of PET is 2.596 g of H₂BDC

[26, 38], and W_{precipitate} is the weight of H₂BDC extracted from designed experiments.

2.3 Experimental design for hydrolysis reaction using RSM

RSM is a crucial statistical tool for optimizing experimental parameters and minimizing the number of investigations. It effectively optimizes, maximizes, or minimizes output responses influenced by multiple input factors [39, 40]. The interactive effects of essential input variables on the output response are simulated through RSM. Within RSM, the Box-Behnken design (BBD) holds significance for evaluating quadratic response surfaces and developing second-order polynomial models. The BBD is a spherical, 3-level fractional factorial design, including a central point and the middle points on the edges of a circumscribed circle [41]. In this research, NaOH concentration, temperature, and time are critical factors influencing the extraction efficiency of H₂BDC from PET waste. The BBD method is employed to determine the optimum conditions for PET waste hydrolysis using the hydrothermal method in an autoclave. The experimental design incorporates three levels of BBD (-1, 0, +1) with 17 tests and five duplications at the central point. NaOH concentration, temperature, and time are independent variables, while H₂BDC yield is the response variable [26]. These values are determined based on prior research outcomes and preliminary screening experiments, ensuring comprehensive parameter space coverage [26, 42]. For instance, NaOH concentrations ranging from 5 to 15%, temperatures spanning from 160 to 200 °C, and hydrolysis times varying from 8 to 12 h are considered (as detailed in Table S2). Utilizing Minitab software version 20 further facilitates the analytical process, aiding in data interpretation and model development. This systematic approach not only streamlines the optimization process but also enhances the overall robustness of the experimental design. The RSM experimental results are fitted using the second-order polynomial equation, represented as Eq. (3) [26, 43].

$$Y = \beta_0 + \sum_{i=1}^3 \beta_i X_i + \sum_{i=1}^3 \beta_{ii} X_i^2 + \sum_{i < j}^n \beta_{ij} X_i X_j + \varepsilon \tag{3}$$

where Y is the predicted response, X_i and X_j are independent variables; β₀ is an intercept coefficient, β_i is a linear coefficient, β_{ii} is a quadratic coefficient; β_{ij} is an interactive coefficient; n is the number of independent variables, ε is the experimental error. Variance (ANOVA) analysis is conducted to assess the statistical significance of the polynomial model at a 95% confidence level and to reveal the interaction between independent variables and the response variable.

2.4 Characterization

The elemental composition of PET samples and H₂BDC production are analyzed using an elemental analyzer (Vario MICRO Elementary Analyzer). The energy content of PET samples is determined by a bomb calorimeter (Parr 1341 calorimeter, NIEA E214.01C). H₂BDC diffraction profiles are obtained through X-ray diffraction (XRD, Bruker, D8, Advance) with CuK α radiation ($\lambda=1.5406 \text{ \AA}$) at a scan rate of $0.03^\circ \text{ s}^{-1}$ and the 2θ range of $5\text{--}80^\circ$. Fourier transform infrared (FTIR) spectra (Frontier MIR/FIR) are recorded in the wavelength range of $650\text{--}4,000 \text{ cm}^{-1}$ with a high resolution of 0.4 cm^{-1} . Nuclear magnetic resonance (NMR) spectroscopy (Varian 500 NMR spectrophotometer) is employed to gather structural information regarding hydrogen and assess the purity of the H₂BDC production yield. The morphological characteristics of H₂BDC are examined using field emission-scanning transmission electron microscopy (FE-SEM, Leica, Stereoscan 420).

3 Results and discussion

3.1 Optimization of the hydrolysis process using the RSM

3.1.1 Development of regression model

The preliminary results of the H₂BDC extraction from PET waste are presented in Table S2, revealing that the conversion of PET and the yield of H₂BDC were significantly influenced by NaOH concentration, reaction temperature, and time. The highest H₂BDC production yield

of $97 \pm 1\%$ was obtained under 10% NaOH, temperature 200°C , and 12 h, while the lowest yield of $38 \pm 3\%$ occurred at 5% NaOH, temperature 160°C , and 10 h. A hydrolysis reaction without alkanile was conducted to understand the role of NaOH in PET hydrolysis further. The result indicated that the recovery ratio was only about 18.7%, highlighting the crucial role of NaOH in hydrolysis (as shown in Table S2). Notably, the TBAI catalyst did not significantly enhance H₂BDC extraction efficiency from PET flake, and citric acid demonstrated superior potential in precipitating H₂BDC compared to sulfuric acid, resulting in a high H₂BDC production yield. The study also revealed that DI water could replace ethanol in washing H₂BDC production (as indicated in Table S2 and Fig. S1), with the ¹H-NMR spectrum in Fig. S1 confirming identical purity using ethanol and DI water.

The results presented in Table S2 provided a valuable basis for selecting and designing the experimental conditions of independent variables for the RSM. The experimental results obtained under various designed conditions of independent variables were used to establish the regression model (as shown in Table 1). The statistical parameters in Table S3 demonstrated that the quadratic model best predicted the H₂BDC yield, supported by a high predicted R-squared ($R\text{-pred}=0.961$), a very low P -value (<0.0001), and a small predicted residual error sum of squares (PRESS*) of 178. The

Table 1 Comparison results between experimental and predicted of H₂BDC yield and recovery rate by Box-Behnken matrix

Independent variables			H ₂ BDC yield (%)			Recovery ratio (%)		
NaOH (%)	Temperature (°C)	Time (h)	Experimental	Predicted	Residual	Experimental	Predicted	Residual
10	200	12	97±1	98	-1	98	100	-2
10	180	10	75±1	74	1	72	71	1
5	200	10	91±1	90	1	92	91	1
15	200	10	97	97	-0	100	99	1
15	180	8	96±1	96	-1	100	100	0
5	180	8	52±3	54	-2	53	54	-1
5	160	10	38±3	38	0	33	34	-1
10	160	8	67±2.0	65	2	68	65	3
15	180	12	95±1	94	1	100	99	1
10	180	10	72±2	74	-2	72	71	1
10	180	10	76±1	74	2	74	71	3
10	200	8	91±2	91	0	94	93	1
10	160	12	70±2	71	-1	72	73	-1
15	160	10	96±1	97	-1	100	100	0
5	180	12	71±2	70	1	74	72	2
10	180	10	74±2	74	0	70	71	-1
10	180	10	73±2	74	-1	69	71	-2
5	200	12	99	100	-1	100	100	0

quadratic model also indicated the highest determination coefficient (R-squared=0.995) and the smallest value of PRESS* compared to other models (as depicted in Table S3), explaining 99.5% of the response variability.

The reliability of the quadratic model was evaluated using statistical parameters and an ANOVA table, as presented in Table S4. The F-value of 195 indicated a significant difference in the means of other groups, making this model highly significant. The P-value for H₂BDC production yield was less than 0.0001, and the "Prob > F" values for almost all terms in Table S4 were less than 0.05, indicating the statistical significance of the quadratic model and its terms at the 95% confidence level. The Lack of Fit F-value was 2.06, which was more significant than 0.05, indicating its insignificance, with only a 25.1% chance that the Lack of Fit F-value could be attributed to noise [26, 44]. The R-sq(adj) of 0.989 and R-sq(Pred) of 0.961 were not significantly different, suggesting that the quadratic model can effectively navigate the design range. The variance inflation factor of 1.00, obtained from the RSM result using Design of Experiments, demonstrated the independence of variables in the quadratic model. In summary, the statistical results of the quadratic model are highly significant and adequate for interpreting experimental data. Therefore, the quadratic regression equation for studying H₂BDC yield is as follows Eq. (4):

$$\text{Yield}(\%) = 64.2 + 30.27X_1 - 2.135X_2 - 6.80X_3 + 0.0730X_1^2 + 0.01141X_2^2 + 0.669X_3^2 - 0.13120X_1X_2 - 0.4834X_1X_3 \quad (4)$$

X₁, X₂, and X₃ are symbols of NaOH concentration (%), temperature (°C), and time (h), respectively. Yield (%) is H₂BDC production.

3.1.2 Proposed regression model analysis

The adequacy of the proposed quadratic model was further evaluated through Fig. 2 and S2. The normality assumption of the model was validated by the bell-shaped histogram of residuals illustrated in Fig. S2. Figure 2a presented the H₂BDC yield obtained from experimental observations was compared with the quadratic regression model, revealing a commendable agreement between the experimentally observed and predicted values. This demonstrates that the proposed quadratic model can accurately predict the experimental results [45, 46]. Moreover, Fig. 2b showed that the difference between internally studentized residuals and predicted responses remained within the 2.0 range without any abnormal observations, confirming that the experimental data were suitable for the predicted ones calculated from Eq. (2). The normal probability percent and residuals are presented in Fig. 2c, where residuals were employed to examine the

assumption of intimate variance. The uniform scattering of data about both sides of the line suggests the appropriateness of the proposed model for this study. The diagnostic plot points closely resembled a straight-line model, with no necessity for data smoothing. Consequently, the proposed quadratic model is deemed adequate for predicting experimental results.

3.1.3 Optimum condition and interactive effects between variables using Pareto chart and three-dimensional response surface

The BBD was implemented in this research to optimize the independent variables, including NaOH concentration, temperature, and time, to achieve maximum H₂BDC yield and recovery ratio. Desirability served as a criterion factor for selecting each independent parameter, with desirability value ranges between 0 (indicating an utterly undesirable response) and 1 (representing a highly desirable response). The BBD optimization results, illustrated in Fig. S3, suggest that the optimal conditions for 5% NaOH concentration, temperature (200 °C), and time (12 h) yielded a maximum H₂BDC yield and recovery ratio of 100%, with a desirable value of 1.00. The model-based H₂BDC yield closely aligned with experimental observations at 99% (Residual of 1.3 as indicated in Table 1), and there was no significant difference between model-

based H₂BDC recovery ratio and experimental values at the optimum conditions. Thus, it can be concluded that RSM is an efficient approach for optimizing PET waste hydrolysis. Figures 2d and e present the standardized effects of independent variables on H₂BDC production yield and recovery ratio. NaOH concentration exhibited a more significant effect than temperature and time, with temperature having a more significant effect than time (as shown in Figs. 2d, e, and S4). The interaction between NaOH concentration and temperature was more prominent than between NaOH and time. However, the interactive effect of temperature and time on H₂BDC yield and recovery ratio was insignificant (as shown in Fig. S5). 3D response surface plots in Fig. 3 reveal the interaction among independent variables and their effects on H₂BDC yield and recovery ratio. Based on the proposed quadratic response equation, the plots demonstrate a significant increase in H₂BDC yield and recovery ratio with higher NaOH concentration, temperature, and reaction time. However, a slight decrease in production yield and recovery ratio was observed at a constant 15% NaOH concentration when the time was increased from 8 to 10

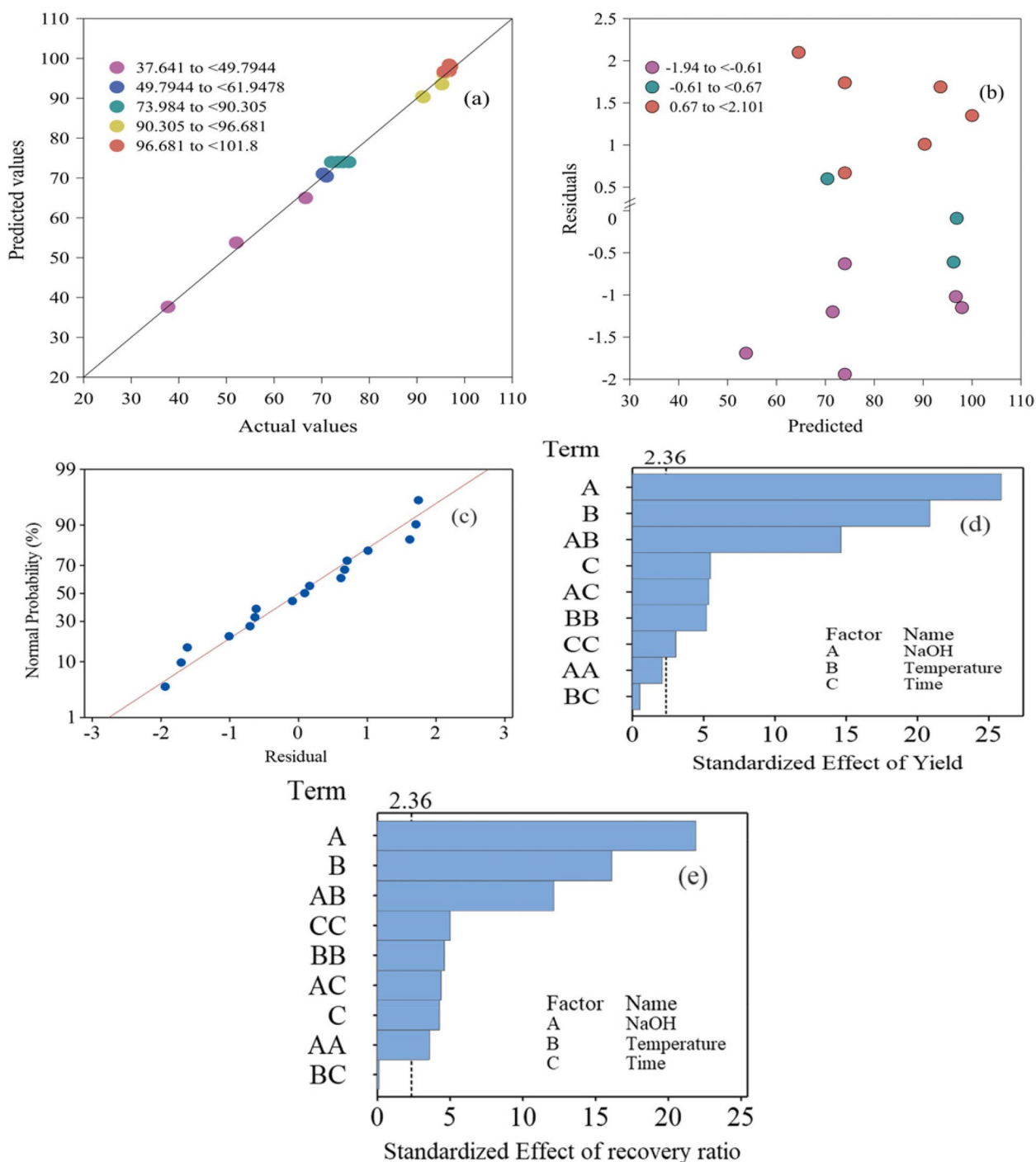


Fig. 2 Predicted plots of H₂BDC yield: **a** actual and predicted values of the quadratic model; **b** Internally studentized residuals vs. predicted values; **c** Normal probability and internally studentized residual for H₂BDC yield; **d** Pareto charts of standardized effects for H₂BDC yield; and **e** Pareto charts of standardized effects for H₂BDC recovery ratio

h at higher temperatures (160 and 180 °C) (as shown in Fig. S6). This could be attributed to the higher evaporation of DI water at higher temperatures, which reduces water molecules and increases NaOH concentration.

As water is essential in promoting PET hydrolysis [11, 12], a decrease in water molecules can negatively affect the hydrolysis process and consequently decrease the H₂BDC yield and recovery ratio. Therefore, it is crucial

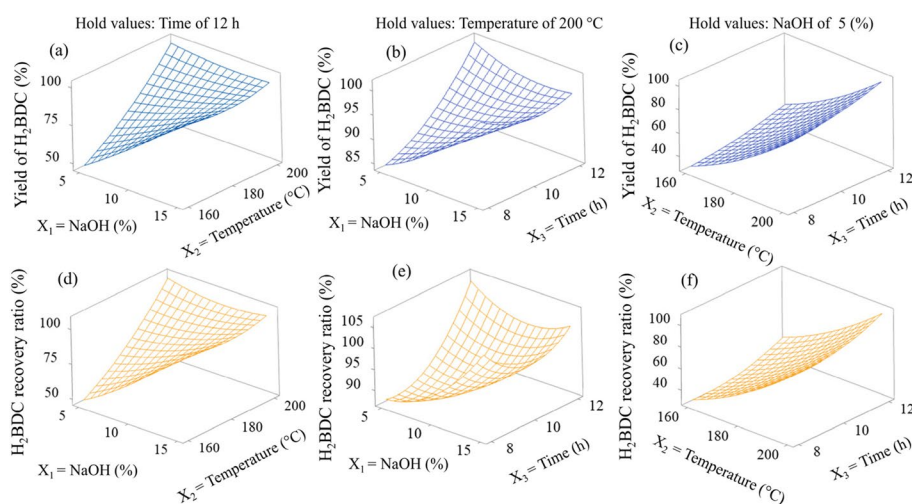


Fig. 3 3D response surface plots for H₂BDC yield (a, b, and c) and recovery ratio (d, e, and f) illustrating the interactive effects at optimization solution: a and d NaOH and temperature; b and e: NaOH and time; c and f temperature and time

to determine the optimum NaOH dosage corresponding to temperature and time to avoid setting up beyond the optimum conditions. The study determined the optimum PET: water mass ratio as 1:10, aligning with previous studies [12, 26]. Analyzing results through a Pareto chart emphasizes the significant influence of NaOH on the H₂BDC production yield and recovery ratio, followed by temperature and time (as shown in Figs. S4, S5, and S7). Thus, under optimal conditions (200 °C for 12 h), the depolymerization of 2.0 g of PET waste achieved 1.72 g of H₂BDC. This process consumed 6 mL of 5% NaOH solution and 20 mL of DI water to hydrolyze PET waste and 2 mL of 20% NaOH solution to neutralize the hydrolysis mixture. In conclusion, RSM proved effective in determining optimum conditions and interactive effects of variables for the PET waste hydrolysis process.

3.2 Optimum conditions of the acidification stage

3.2.1 The efficiency of sulfuric acid and citric acid for H₂BDC precipitation

The precipitation reactions were conducted under the same ambient temperature conditions, reaction time (with a slow feeding rate over 40 min), and agitation speed of 300 rpm. To gain 1.72 g of H₂BDC from acidification reactions of the hydrolyzed mixture, which consumed approximately 8.5 mL 4.5 M H₂SO₄ or 20 mL 4.5 M C₆H₈O₇ to adjust the pH to 1.0 and 4.0, respectively. Then, the product was washed thrice with 30 mL of DI water. Figure 4 illustrates the PXRD spectra and SEM images of PET-derived H₂BDC precipitated by 4.5 M citric acid and sulfuric acid. The results indicated an insignificant difference in H₂BDC yield and recovery ratio between citric and sulfuric acid. However, H₂BDC

precipitated with citric acid exhibited superior quality and characteristics compared to sulfuric acid, as shown in Fig. 4a. Remarkably, the particle size of H₂BDC produced using citric acid was approximately 10.4 μm, which is larger than that produced by sulfuric acid in Fig. 4b. Additionally, the diffraction peaks obtained using citric acid for H₂BDC precipitation were sharper and stronger than those obtained using sulfuric acid. These results suggest that the H₂BDC crystals precipitated with citric acid were more well-defined and ordered, indicating higher crystallinity. It is important to note that strong acids such as H₂SO₄ or HCl pose safety and corrosion concerns, leading to elevated environmental pressure and increased production costs. In contrast, citric acid is a more environmentally friendly alternative. Moreover, the pH of wastewater after the precipitation period was lower when using sulfuric acid (pH=2.0) compared to using citric acid (pH=5.0). To further compare the precipitation performance by H₂SO₄ and citric acid, the nitrate levels were 0.5 mg L⁻¹ for H₂SO₄ and 0.04 mg L⁻¹ for citric acid, respectively. However, it is important to note that using citric acid for neutralizing and precipitating H₂BDC not only is more eco-friendly but also results in a significantly higher quality and larger particle size of H₂BDC as compared to sulfuric acid.

3.2.2 Optimum conditions for H₂BDC particle size and yield at the acidification stage

This research determined a final pH value of 4.0 for the precipitation reaction, as the H₂BDC yield showed no significant difference between pH 2.5 and 4.0. To obtain 1.72 g of H₂BDC from the acidification reactions of the hydrolyzed mixture using a combination of DMSO and

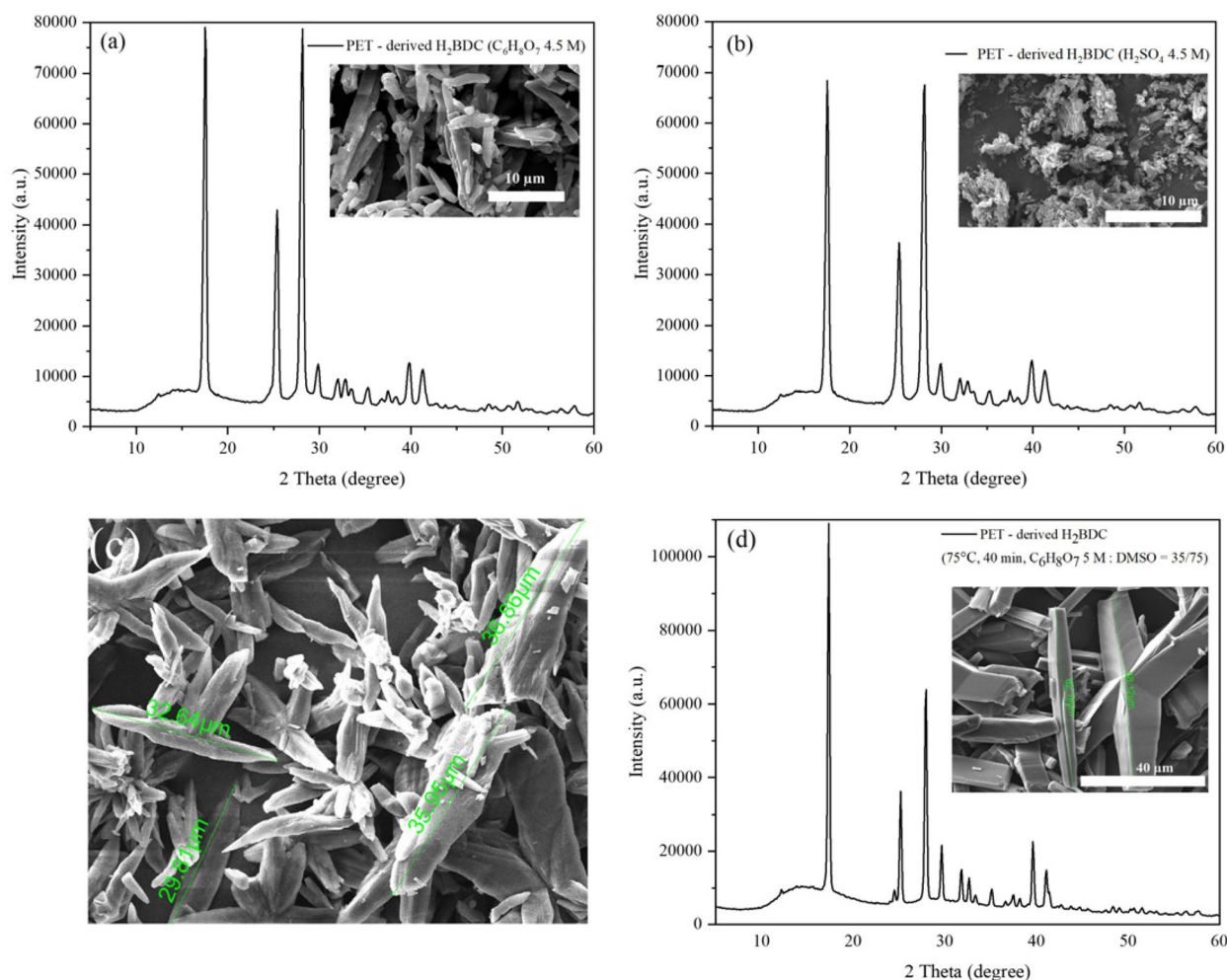


Fig. 4 PXRD spectra and SEM image of PET-derived H₂BDC precipitated by (a) C₆H₈O₇ (4.5 M) in 40 min; (b) by H₂SO₄ (4.5 M) in 40 min; (c) (C₆H₈O₇ 5 M/DMSO (1:1), 25 °C, 40 min); (d) ((C₆H₈O₇ 5 M/DMSO = 35/75 mL), 75 °C, 40 min)

citric acid, which consumed approximately 35 mL 5 M C₆H₈O₇ and 75 mL DMSO were utilized to adjust the pH to 4.0. Subsequently, the product was washed with 30 mL DI water. Particle size, a critical factor for H₂BDC production quality [17], was enhanced using citric acid mixed with DMSO. Figure 4c displays H₂BDC particle size under precipitation conditions, where 15 mL 5 M C₆H₈O₇ was remixed with 15 mL DMSO at 25 °C for 40 min. Experimental results showed a significant improvement in H₂BDC particle size from 10.4 to 33.2 μm (as shown in Fig. 4a and c), while yield remained insignificantly about 97%. This occurrence arises due to the water-insolubility of H₂BDC, resulting in its rapid precipitation and subsequent formation of fine particles. Citric acid was mixed with DMSO to achieve a slow degree of supersaturation and increase the equilibrium concentration of H₂BDC, resulting in larger crystals.

The study found that acid concentration, reaction time, and temperature significantly influenced H₂BDC particle size but did not affect yield. In the case of ambient temperature and 40 min minutes of reaction time, the particle size increased from 13.5 to 33.2 μm with an increase in the C₆H₈O₇ concentration from 1 to 5 M (as indicated in Table S5, Figs. S8a and S8b). This phenomenon can be attributed to the fact that the C₆H₈O₇ concentration increases, leading to a reduction in the ratio of the aqueous phase to DMSO and an increase in dissolved H₂BDC in DMSO. However, in the case of the relatively high C₆H₈O₇ concentration (6 M), the particle size significantly decreased from 11.2 to 3.6 μm (Figs. S8c and S8d), resulting in a sudden jump in supersaturation from the instant conversion of Na₂-H₂BDC into H₂BDC and rapid nucleation. Therefore, 5 M C₆H₈O₇ was deemed suitable for obtaining the desired particle size of H₂BDC.

Table 2 Comparison results of PET-derived H₂BDC extraction efficiency

PET size	Depolymerization process				Precipitation process			H ₂ BDC production		Ref
	Agent	T (°C)	Time (h)	Catalyst	Heating	Acid	PT (min)	Yield/ Recovery ratio (%)	Particle size (µm)	
Flakes	NaOH (5%)	200	12	No	Autoclave	C ₆ H ₈ O ₇ / DMSO	40	99/100	57.39	This study
Flakes	NaOH (14.5%)	200	5	No	Autoclave	H ₂ SO ₄ / DMSO	55	92	25	[28]
Flakes	EG	190	3	No	Microwave	2 M H ₂ SO ₄	ND	87	ND	[37]
Flakes	EG	210	8	No	Autoclave	ND	ND	55	ND	[31]
Granules	TPA	220	4	TPA	Pressure-tight reactor	H ₂ SO ₄	ND	96/100	ND	[12]
Granules	ZSM-5	230	0.5	ZSM-5	Microwave	2 M HCl	ND	97/99	ND	[11]
Granules	NaOH (4%)	110	12	CTAB	Autoclave	1 M H ₂ SO ₄	ND	90/89	ND	[49]
Powder	NaOH (14.5%)	83	1.5	TBAI	Ultrasonicator	H ₂ SO ₄	ND	100	ND	[26]
Powder	NaOH (10%)	90	1	TBAI	Microwave	HCl	ND	98	ND	[50]

ND Not detected, TBAI/Tetrabutylammonium iodide, EG Ethylene glycol, T temperature, PT Precipitation time, CTAB cetyltrimethylammonium bromide

By increasing the reaction time from 5 to 40 min, a significant increase in particle size from very fine to 11.2 μm was observed under the slower feeding speed and the same conditions (25 °C and 5 M citric acid concentration) (as shown in Figs. S8d and S8e), 5 min of reaction time resulted in fast precipitation and a sudden rise in supersaturation while 40 min allowed for the assembly of H₂BDC solubles into larger crystals. However, H₂BDC particle size did not significantly differ under 40 and 60 min of reaction time. The study highlighted that reaction temperature during the acidification step significantly affects particle size (as shown in Fig. 4d). The mixture of DMSO and 5 M C₆H₈O₇ promoted the largest particle size and crystallinity at 75 °C, with an average particle size of 57.4 μm . This phenomenon can be ascribed to the significant solubility of H₂BDC in DMSO at 75 °C. The H₂BDC particle size produced is larger than reported by previously published literature [28] (as indicated in Table 2). Therefore, this study creates a large H₂BDC particle size, preventing product loss and saving energy during filtration and drying. Larger crystals have lower moisture content, allowing for a drying temperature and time of 60 °C in 12 h for this study, compared to fine particles that require 90 °C for 24 h [47] or 100 °C for 24 h [5]. In summary, the optimum conditions for particle size and yield of H₂BDC at the hydrolysis and precipitation stages were recorded as follows: a PET: H₂O mass ratio of 1:3, NaOH (5%), 200 °C, and the reaction time of 12 h for the hydrolysis stage, and the 5 M C₆H₈O₇: DMSO volume ratio of 1:2 (35 mL C₆H₈O₇ mixed with 75 mL DMSO), 75 °C with a reaction time of 40 min and 300 rpm during the precipitation stage.

3.3 Reusability test of the mixture of citric acid and DMSO

Reusing the citric acid and DMSO mixture from the H₂BDC precipitation process is crucial for the subsequent acidification reaction. By reusing this mixture, extraction costs are minimized, and wastewater generation is avoided, reducing the demand for further treatment. After cooling the reaction solution to room temperature, filtration is employed to recover H₂BDC and separate the aqueous solution. The aqueous phase, which contains citric acid and DMSO, serves as the reaction solution for the subsequent acidification process. Assessing the reusability of the citric acid and DMSO mixture involves evaluating the yield, particle size, and purity of the produced H₂BDC. The chemical structure of produced H₂BDC was determined using ¹H and ¹³C NMR spectroscopy. The results depicted in Fig. 5a–c illustrate that the spectra of H₂BDC remain consistent after eight cycles, aligning with the commercial H₂BDC and initial cycle. Consequently, the chemical structure and purity of H₂BDC remain unchanged. In addition, the

particle size exhibits a slight change after eight cycles, ranging from 47.1 to 60.1 μm , as shown in Fig. 5d. The yield of produced H₂BDC remains stable, maintaining between 96 to 99% over eight cycles of continuous reuse. It suggests that recycling the citric acid and DMSO mixture has no detrimental effect on the purity and yield of H₂BDC. Thus, DMSO retains its high potential for enhancing the particle size of H₂BDC over eight cycles of the aqueous phase.

3.4 Evaluation of PET-derived H₂BDC quality at optimum conditions

FTIR analysis was employed to determine the chemical structure of PET waste, PET-derived H₂BDC, and commercial H₂BDC, as illustrated in Fig. 6a. The peaks observed at 1,578, 1,511, and 1,422 cm⁻¹ are attributed to the benzene ring vibration of H₂BDC and PET [25]. Peaks around 1,282 and 2,548–3,062 cm⁻¹ correspond to the stretching vibrations of carboxylic groups [16]. The peak at 1,678 cm⁻¹ signified the carbonyl groups' stretching vibration, while the 728 cm⁻¹ peak indicated the out-of-plane bending vibrations of aromatic rings [26, 48]. Peaks at 1,730 and 1,252 cm⁻¹ in the original PET spectra are attributed to the stretching vibrations of C=O and C-O of the ester bonds, respectively. A remarkable feature in Fig. 6a is the presence of identical characteristic peaks between PET-derived H₂BDC and commercially produced H₂BDC, confirming the successful recovery of H₂BDC from PET bottles. The PXRD diffraction spectra in Fig. 6b exhibit multiple sharp Bragg and strong diffraction peaks at 17.2, 25.3, 27.9, 29.8, and 39.8°, indicating high crystallinity of PET-derived H₂BDC. Characteristic peaks for PET-derived H₂BDC and commercial H₂BDC coincide well and are consistent with previously reported studies [5, 26, 31].

Furthermore, NMR spectroscopy was conducted to analyze the chemical structure and purity of PET-derived H₂BDC, as shown in Fig. 5a. In the ¹H NMR spectra, peaks at 8.04 and 13.29 ppm are attributed to the aromatic protons of the benzene ring and the hydroxyl protons, respectively. The ¹³C NMR spectra displayed signals at 129.38, 134.41, and 166.58 ppm, corresponding to the aromatic (C^A), quaternary aromatic (C^B), and carbonyl (C^C) carbon atoms of H₂BDC. The PET-derived H₂BDC spectra match well with ¹H NMR and ¹³C NMR spectra of commercial H₂BDC (as shown in Fig. 5a and b) and align with previously published results [9, 25]. No other peaks, except those from the NMR solvent, were observed, indicating the high purity of the produced H₂BDC. The elemental analysis results showed that carbon content in commercial H₂BDC production and PET-derived H₂BDC production were 58 ± 0.37% and

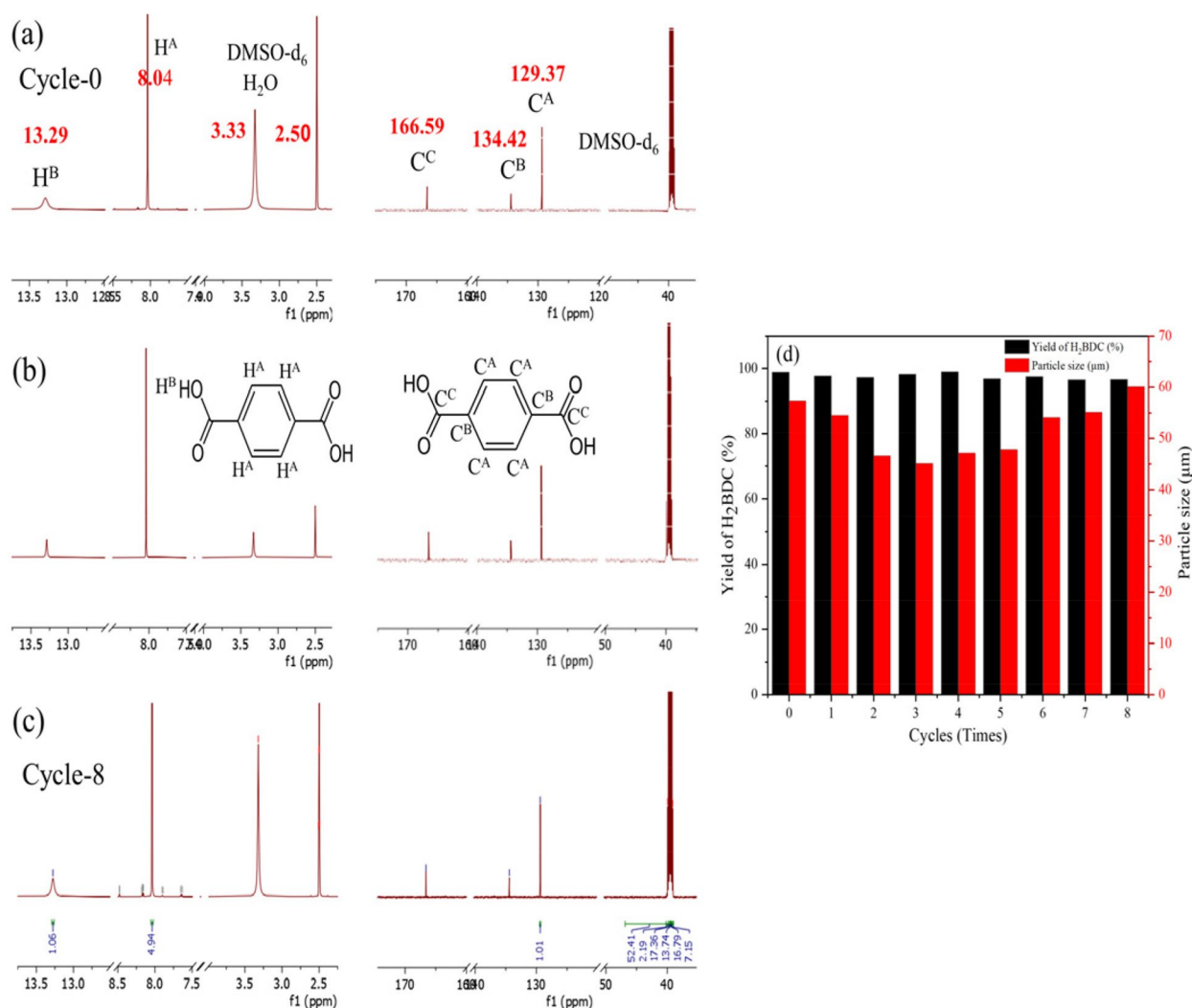


Fig. 5 ¹H and ¹³C NMR spectra of (a) PET-derived H₂BDC of cycle-0; (b) commercial H₂BDC; (c) PET-derived H₂BDC of cycle-8; (d) The effect of recycling the aqueous phase on the yield and particle size of H₂BDC

57 ± 1.90%, respectively. Meanwhile, the hydrogen content of H₂BDC from commercial H₂BDC and PET-derived processes were quite similar, ranging between 3.7 ± 0.12% and 3.5 ± 0.08%, respectively. These findings affirm that PET-derived H₂BDC has a consistent structure, quality, and purity comparable to commercial H₂BDC (purity: 99%), making it suitable for commercial development.

Table 2 compares the extraction efficiency of PET-derived H₂BDC under optimal conditions in this study with values reported in previous studies [11, 12, 26, 28, 31, 37, 49, 50]. Notably, particle size plays a crucial role in determining the production quality of PET-derived H₂BDC, impacting its compliance with commercial

product standards. However, several previous studies have overlooked critical parameters such as precipitation time and particle size. The current research has made significant advancements, achieving an improved particle size of 57.3 µm and a high yield of 98% by applying a combination of citric acid and DMSO during the acidification step within a short reaction time of 40 min. This result contrasts the report by previous research [17], which used a mixture of sulfuric acid and DMSO, resulting in a particle size of 25 µm and yield (92%) with a reaction time of 55 min. As seen in Table 2, recent researchers have shown interest in using catalysts for hydrolysis and strong acids for acidification, leading to increased operating costs and

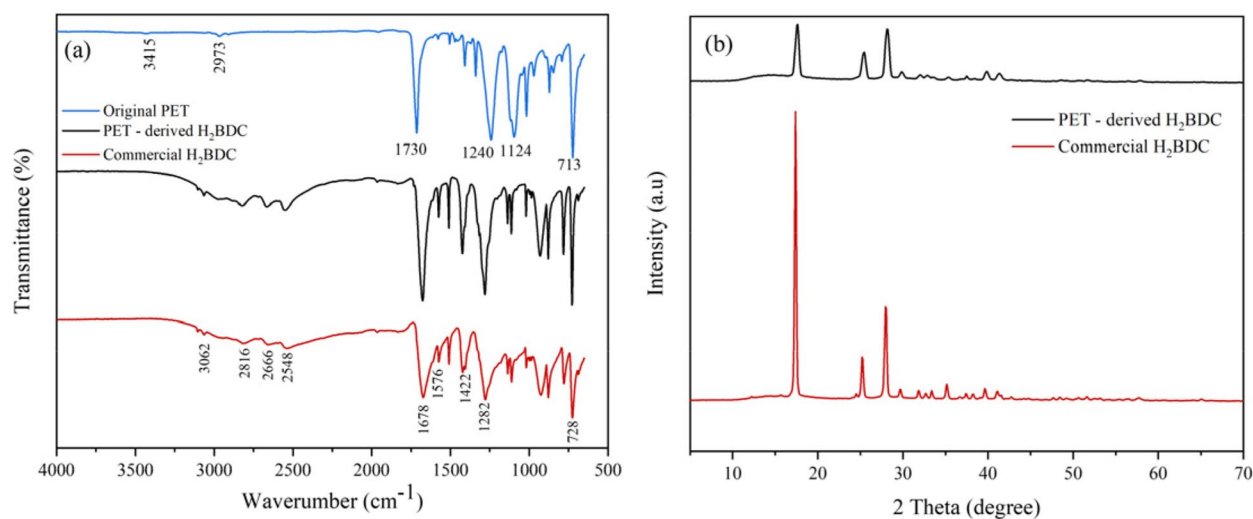


Fig. 6 **a** Comparison FT-IR spectrum of PET-derived H₂BDC vs. commercial H₂BDC and original PET; **b** PXRD pattern of PET-derived H₂BDC vs. commercial H₂BDC

hazardous substrates. In contrast, the current study determined the optimum conditions for hydrolysis and acidification without using catalysts and strong acids, resulting in cost-efficiency and eco-friendly operation.

4 Conclusions

This study successfully identified the optimal conditions for PET hydrolysis using hydrothermal processes, specifically at 200 °C for 12 h with 5% NaOH. It represents a significant step forward by enhancing the quality of PET waste-derived H₂BDC and reducing pollutant concentrations in wastewater resulting from the acidification process. A unique combination of citric acid and DMSO was used in this research to precipitate H₂BDC from the hydrolyzed PET mixture. This innovative method substantially improved the particle size of H₂BDC, meeting commercial production standards. Key insights from the experiments highlighted the critical role of DMSO in controlling the particle size of H₂BDC. Notably, the results showed that the reuse of the DMSO and citric acid mixture did not compromise the quality or yield of H₂BDC production. The method's environmentally friendly and cost-effective nature, utilizing benign precursors and promoting high reusability of the citric acid and DMSO mixture, underscores the sustainability of the process. Consequently, this study addresses the limitations of prior research that relied on strong acids and catalysts without determining the optimal hydrolysis conditions or considering the reuse of acid and the particle size of H₂BDC during

the acidification process. In summary, the findings highlight the promising potential for industrializing H₂BDC derived from PET, offering an environmentally conscious and economically viable pathway for its production. Future research will focus on applying PET waste-derived H₂BDC to synthesize various MOFs and evaluating their capacity for adsorption and separating contaminants in water, wastewater, and air research fields.

Supplementary Information

The online version contains supplementary material available at <https://doi.org/10.1186/s42834-024-00220-2>.

Supplementary Material 1.

Acknowledgements

The authors would like to thank the National Science and Technology Council (NSTC) Taiwan for financially supporting this work (Grand No. NSTC-111-2221-E-008-012-MY3). The authors also appreciate the Precious Instruments Utilization Center of National Central University in providing analysis facilities.

Authors' contributions

Thi Hong Nguyen is the first author responding to collect, analyze data, and write a draft manuscript. Prof Kung-Yuh, Chiang is the corresponding author who supervised and revised the whole research. All authors have read and approved the final manuscript.

Funding

This research was supported by the Taiwan National Science and Technology Council (NSTC).

Availability of data and materials

The datasets collected and analyzed during this study are mentioned in the submitted article and supplementary materials.

Declarations

Competing interests

The authors declare they have no competing interests.

Received: 20 January 2024 Accepted: 28 June 2024

Published online: 19 July 2024

References

- Gurler N, Pasa S, Temel H. Silane doped biodegradable starch-PLA bilayer films for food packaging applications: Mechanical, thermal, barrier and biodegradability properties. *J Taiwan Inst Chem E*. 2021;123:261–71.
- Mendiburu-Valor E, Mondragon G, Gonzalez N, Kortaberria G, Martin L, Eceiza A, et al. Valorization of urban and marine PET waste by optimized chemical recycling. *Resour Conserv Recy*. 2022;184:106413.
- Davidson MG, Furlong RA, McManus MC. Developments in the life cycle assessment of chemical recycling of plastic waste – A review. *J Clean Prod*. 2021;293:126163.
- Ko S, Kwon YJ, Lee JU, Jeon YP. Preparation of synthetic graphite from waste PET plastic. *J Ind Eng Chem*. 2020;83:449–58.
- Ren J, Dyosiba X, Musyoka NM, Langmi HW, North BC, Mathe M, et al. Green synthesis of chromium-based metal-organic framework (Cr-MOF) from waste polyethylene terephthalate (PET) bottles for hydrogen storage applications. *Int J Hydrogen Energ*. 2016;41:18141–6.
- Lin CH, Gung CH, Wu JY, Suen SY. Cationic dye adsorption using porous composite membrane prepared from plastic and plant wastes. *J Taiwan Inst Chem E*. 2015;51:119–26.
- Adnan, Shah J, Jan MR. Effect of polyethylene terephthalate on the catalytic pyrolysis of polystyrene: Investigation of the liquid products. *J Taiwan Inst Chem E*. 2015;51:96–102.
- Liu Y, Liao C, Tang Y, Tang J, Sun Y, Ma X. Techno-environmental-economic evaluation of the small-scale municipal solid waste (MSW) gasification-based and incineration-based power generation plants. *J Taiwan Inst Chem E*. 2022;141:104594.
- Alpizar F, Carlsson F, Lanza G, Carney B, Daniels RC, Jaime M, et al. A framework for selecting and designing policies to reduce marine plastic pollution in developing countries. *Environ Sci Policy*. 2020;109:25–35.
- d'Ambrieres W. Plastics recycling worldwide: current overview and desirable changes. *Field Actions Sci Rep*. 2019;19:12–21.
- Kang MJ, Yu HJ, Jegal J, Kim HS, Cha HG. Depolymerization of PET into terephthalic acid in neutral media catalyzed by the ZSM-5 acidic catalyst. *Chem Eng J*. 2020;398:125655.
- Yang W, Liu R, Li C, Song Y, Hu C. Hydrolysis of waste polyethylene terephthalate catalyzed by easily recyclable terephthalic acid. *Waste Manage*. 2021;135:267–74.
- Kusumocahyo SP, Ambani SK, Kusumadewi S, Sutanto H, Widiputri DI, Kartawiria IS. Utilization of used polyethylene terephthalate (PET) bottles for the development of ultrafiltration membrane. *J Environ Chem Eng*. 2020;8:104381.
- Maniyan NH, Parashar K, Kadam LN, Srivastava DN. Electrochemical detection of heat shock protein 70 over cost-effective plastic chip electrode platform. *J Taiwan Inst Chem E*. 2021;128:11–9.
- Rahimi S, Rostamizadeh M. Novel Fe/B-ZSM-5 nanocatalyst development for catalytic cracking of plastic to valuable products. *J Taiwan Inst Chem E*. 2021;118:131–9.
- Chu M, Liu Y, Lou X, Zhang Q, Chen J. Rational design of chemical catalysis for plastic recycling. *ACS Catal*. 2022;12:4659–79.
- Martin AJ, Mondelli C, Jaydev SD, Perez-Ramirez J. Catalytic processing of plastic waste on the rise. *Chem*. 2021;7:1487–533.
- Hao L, Liu N, Zhang B, Niu R, Gong J, Tang T. Waste-to-wealth: Sustainable conversion of polyester waste into porous carbons as efficient solar steam generators. *J Taiwan Inst Chem E*. 2020;115:71–8.
- Li H, Aguirre-Villegas HA, Allen RD, Bai X, Benson CH, Beckham GT, et al. Expanding plastics recycling technologies: chemical aspects, technology status and challenges††Electronic supplementary information (ESI) available. *Green Chem*. 2022;24:8999–9002.
- George N, Kurian T. Recent developments in the chemical recycling of postconsumer poly(ethylene terephthalate) waste. *Ind Eng Chem Res*. 2014;53:14185–98.
- Geyer B, Lorenz G, Kandelbauer A. Recycling of poly(ethylene terephthalate) – a review focusing on chemical methods. *Express Polym Lett*. 2016;10:559–86.
- Glaser JA. New plastic recycling technology. *Clean Technol Envir*. 2017;19:627–36.
- Shen L, Worrell E. Plastic recycling. In: Meskers C, Worrell E, Reuter MA, editors. *Handbook of Recycling*. 2nd Ed. Amsterdam: Elsevier; 2024, p. 497–510.
- Han M. Depolymerization of PET bottle via methanolysis and hydrolysis. In: Thomas S, Rane A, Kanny K, Abitha VK, Thomas MG, editors. *Recycling of Polyethylene Terephthalate Bottles*. Norwich: William Andrew; 2019, p. 85–108.
- Yaashikaa PR, Kumar PS, Nhung TC, Hemavathy RV, Jawahar MJ, Neshaan-thini JP, et al. A review on landfill system for municipal solid wastes: Insight into leachate, gas emissions, environmental and economic analysis. *Chemosphere*. 2022;309:136627.
- Jung KW, Kim JH, Choi JW. Synthesis of magnetic porous carbon composite derived from metal-organic framework using recovered terephthalic acid from polyethylene terephthalate (PET) waste bottles as organic ligand and its potential as adsorbent for antibiotic tetracycline hydrochloride. *Compos Part B-Eng*. 2020;187:107867.
- ASTM. Standard Specification for Woven Wire Test Sieve Cloth and Test Sieves (ASTM E11–22). West Conshohocken: American Society for Testing and Materials International; 2022.
- Lee HL, Chiu CW, Lee T. Engineering terephthalic acid product from recycling of PET bottles waste for downstream operations. *Chem Eng J Adv*. 2021;5:100079.
- Yang WC. *Handbook of Fluidization and Fluid-Particle Systems*. Boca Raton: CRC Press; 2003.
- Karayannidis GP, Achillas DS. Chemical recycling of poly(ethylene terephthalate). *Macromol Mater Eng*. 2007;292:128–46.
- Ghosh A, Das G. Facile synthesis of Sn(II)-MOF using waste PET bottles as an organic precursor and its derivative SnO₂ NPs: Role of surface charge reversal in adsorption of toxic ions. *J Environ Chem Eng*. 2021;9:105288.
- Zhang F, Chen S, Nie S, Luo J, Lin S, Wang Y, et al. Waste PET as a reactant for lanthanide MOF synthesis and application in sensing of picric acid. *Polymers*. 2019;11:2015.
- Martinez A, Vargas R, Galano A. Citric acid: a promising copper scavenger. *Comput Theor Chem*. 2018;1133:47–50.
- Setiawan WK, Chiang KY. Eco-friendly rice husk pre-treatment for preparing biogenic silica: gluconic acid and citric acid comparative study. *Chemosphere*. 2021;279:130541.
- Han H, Yin W, Wang D, Zhu Z, Yang B, Yao J. New insights into the dispersion mechanism of citric acid for enhancing the flotation separation of fine siderite from hematite and quartz. *Colloid Surface A*. 2022;641:128459.
- Deleu WPR, Stassen I, Jonckheere D, Ameloot R, De Vos DE. Waste PET (bottles) as a resource or substrate for MOF synthesis. *J Mater Chem A*. 2016;4:9519–25.
- Manju, Kumar Roy P, Ramanan A, Rajagopal C. Post consumer PET waste as potential feedstock for metal organic frameworks. *Mater Lett*. 2013;106:390–2.
- Paliwal NR, Mungray AK. Ultrasound assisted alkaline hydrolysis of poly(ethylene terephthalate) in presence of phase transfer catalyst. *Polym Degrad Stab*. 2013;98:2094–101.
- Xu Y, Li X, Zhang W, Jiang H, Pu Y, Cao J, et al. Zirconium(IV)-based metal-organic framework for determination of imidacloprid and thiamethoxam pesticides from fruits by UPLC-MS/MS. *Food Chem*. 2021;344:128650.
- Doan KQT, Chiang KY. Statistical optimization of cellulose nanocrystal from cotton cloth waste using sulfuric acid hydrolysis and response surface methodology. *Int J Environ Sci Te*. 2024;21:5691–704.
- Kumari M, Gupta SK. Response surface methodological (RSM) approach for optimizing the removal of trihalomethanes (THMs) and its precursor's by surfactant modified magnetic nanoadsorbents (sMNP) - An endeavor to diminish probable cancer risk. *Sci Rep*. 2019;9:18339.
- Dyosiba X, Ren J, Musyoka NM, Langmi HW, Mathe M, Onyango MS. Feasibility of varied polyethylene terephthalate wastes as a linker source

- in metal–organic framework uio-66(zr) synthesis. *Ind Eng Chem Res.* 2019;58:17010–6.
43. Hariharan N, Senthil V, Krishnamoorthi M, Karthic SV. Application of artificial neural network and response surface methodology for predicting and optimizing dual-fuel CI engine characteristics using hydrogen and bio fuel with water injection. *Fuel.* 2020;270:117576.
 44. Guan S, Deng F, Huang SQ, Liu SY, Ai LX, She PY. Optimization of magnetic field-assisted ultrasonication for the disintegration of waste activated sludge using Box–Behnken design with response surface methodology. *Ultrason Sonochem.* 2017;38:9–18.
 45. Alian E, Semnani A, Firooz A, Shirani M, Azmoon B. Application of response surface methodology and genetic algorithm for optimization and determination of iron in food samples by dispersive liquid–liquid microextraction coupled UV–visible spectrophotometry. *Arab J Sci Eng.* 2018;43:229–40.
 46. Mahdavi R, Ashraf Talesh SS. Enhancement of ultrasound-assisted degradation of Eosin B in the presence of nanoparticles of ZnO as sonocatalyst. *Ultrason Sonochem.* 2019;51:230–40.
 47. Dyosiba X, Ren J, Musyoka NM, Langmi HW, Mathe M, Onyango MS. Preparation of value-added metal-organic frameworks (MOFs) using waste PET bottles as source of acid linker. *Sustain Mater Techno.* 2016;10:10–3.
 48. Doan VD, Do TL, Ho TMT, Le VT, Nguyen HT. Utilization of waste plastic pet bottles to prepare copper-1,4-benzenedicarboxylate metal-organic framework for methylene blue removal. *Sep Sci Technol.* 2020;55:444–55.
 49. Wang Y, Wang H, Chen H, Liu H. Towards recycling purpose: Converting PET plastic waste back to terephthalic acid using pH-responsive phase transfer catalyst. *Chinese J Chem Eng.* 2022;51:53–60.
 50. Khalaf HI, Hasan OA. Effect of quaternary ammonium salt as a phase transfer catalyst for the microwave depolymerization of polyethylene terephthalate waste bottles. *Chem Eng J.* 2012;192:45–8.

Publisher's Note

Springer Nature remains neutral with regard to jurisdictional claims in published maps and institutional affiliations.